Monodisperse Polystyrene Latex Particles Functionalized by the Macromonomer Technique

Alexander Búcsi,*,† Jacqueline Forcada,‡ Sébastien Gibanel,§ Valérie Héroguez,§ Michel Fontanille,§ and Yves Gnanou§

Grupo de Ingeniería Química, Departamento de Química Aplicada, Facultad de Ciencias Químicas, Universidad del País Vasco/EHU, Apdo. 1072, 20080 San Sebastián, Spain, and Laboratoire de Chimie des Polymères Organiques, ENSCPB-CNRS-Université Bordeaux 1 (UMR 5629), Avenue Pey-Berland, 33402 Talence Cedex, France

Received September 29, 1997; Revised Manuscript Received January 27, 1998

ABSTRACT: Monodisperse core−shell latex particles functionalized with surface groups that were introduced by the macromonomer technique were obtained by means of a two-step emulsion polymerization process in a batch reactor at 70 °C. In the first step the cores were synthesized by means of a batch emulsion polymerization of styrene (St), and in the second step, the shells were formed by batch emulsion copolymerizations of St and different macromonomers using the seeds obtained previously. Macromonomers were synthesized by anionic "living" polymerization. They are constituted of a poly(ethylene oxide) hydrophilic block and a hydrophobic block or sequence end-fitted with an unsaturation. The latexes were characterized by gravimetry, transmission electron microscopy (TEM), and conductometric titrations to obtain the conversion, the particle size distribution (PSD), and the surface charge density (σ), respectively. The colloidal stability of the cores and final latexes were determined by measuring the critical coagulation concentration (CCC) at two pHs (7 and 2) using KBr as electrolyte. The surface charges of the latexes were moderately low, with corresponding moderately low CCCs. The presence of spacers, confirmed with a disk centrifuge photosedimentometer (DCP) and photon correlation spectrophotometer (PCS), did not increase the CCC. During the CCC measurements, at high electrolyte concentrations, the reduced solubility of the spacer PEO moiety in the solution resulted in its collapse on the particle surface.

Introduction

The use of polymeric materials as carriers of biomolecules able to detect analytes in solution has been common practice from the mid 50s. Singer and Plotz[1] were pioneers in this field, detecting Rh rheumatoid factor. From that, the field known as "reactive latexes" has experienced a continuous development aimed at improving this technique, including the test reliability, quantification of the analyte detected, and automatation of the process.

Progress in the development of new immunodiagnosis tests requires novel polymeric colloids of defined functionality and colloidal stability.

The most recent investigations devoted to immunodiagnosis combine the latest developments in immunology and polymer science. This latter field contributed to the production of new functionalized polymeric colloids able to bond proteins covalently.[2−6] In this way, the possibility of desorption and/or nonspecific adsorption of the protein, that can take place when it is physically adsorbed on the particle surface, is avoided. Moreover, the covalent bonding is produced at one specific part of the protein, and in this way, the active sites remain free, enhancing the sensitivity of the immunodiagnosis test.

With respect to the synthesis of new functionalized colloids or functionalized latex particles able to bond proteins covalently, the choice of the appropriate comonomers makes the formation of latex particles with the desired surface groups possible. Once the particles are synthesized, their surfaces must be characterized. This characterization will indicate their future application.

The uniform size of the latex particles is one of the main requirements from the point of view of their application, the monodispersity of the particles being confirmed by optical methods.

In the search for suitable experimental conditions to obtain particles of a given size, with narrow size distribution, the concentration and type of emulsifier are decisive. Here the use of macromonomers in the polymerization recipes is described and shown to play a significant role, which is the same as that of a polymerizable surfactant. The macromonomers used in this study were constituted of a PEO hydrophilic block and of a hydrophobic block end-fitted with an unsaturation. The latter is meant to anchor the macromonomer to the latex particle, whereas the PEO part is expected to serve as a steric barrier of the particle. For the proposed application that requires functionalized latex particles capable of reacting with the amino groups of biomolecules, the macromonomer to be used should carry either an aldehyde or an acetal function at the end of its hydrophilic block.

The first part of this paper is devoted to the synthesis of such α-functionalized, ω-styryl PEO-based macromonomers. In the second part, the synthesis of reactive polymeric colloids fitted with aldehyde and acetal functionality that is introduced through copolymerization with the above-mentioned macromonomers is described. The characterization and quantification of the surface groups were carried out by conductometric titrations. The colloidal characterization consisted of the determination of the monodispersity of the particle

† On leave from Polymer Institute, Slovak Academy of Sciences, Dúbravská c. 9, 842 36 Bratislava, Slovakia.
‡ Universidad del País Vasco.
§ ENSCPB-CNRS-Universitè Bordeaux 1.

S0024-9297(97)01434-4 CCC: $15.00
Published on Web 03/13/1998

size distributions by transmission electron microscopy and the study of the colloidal stability against electrolytes (critical coagulation concentration, CCC). Electrophoretic mobility (μ_e) offers additional information about colloidal stability of the emulsion by varying the ionic strength of a 1:1 electrolyte or the pH of the suspension medium.

With respect to the application of these new particles in immunodiagnosis that will be reported in a future work, Immunoglobuline anti-CRP (IgG-aCRP) will be bonded to the surface groups and the immunoreaction will be employed to detect CRP antigen.

Experimental Section

Materials. Styrene (Aldrich, 99%) was first distilled over CaH_2 and stirred over the same drying agent for 24 h before being cryodistilled (distillation under vacuum with the flask receiving the distillate maintained at very low temperature). Ethylene oxide (Fluka, purity 99.8%) was stirred over sodium at −30 °C for 3 h and cryodistilled. *p*-(Chloromethyl)styrene (Aldrich, 97%) and 1,1-diphenylethylene (Aldrich, 97%) were stored over CaH_2 and cryodistilled. *N*,*N*,*N*′,*N*′-Tetramethylethylenediamine was stirred over sodium and cryodistilled. 2,2-Diethoxyethanol (Lancaster, 98%) and 3,3-diethoxypropanol (Aldrich, 98%) were stirred over Mg and cryodistilled. Li (Aldrich, 30% dispersion), 2,2,2-trifluoroethanesulfonyl chloride (Aldrich, 99%), Amberlyst 15 (Aldrich), and acetone (SDS, 99.5%) were used as received. Acetaldehyde 3-chloropropyl ethyl acetal and acetaldehyde 3-lithiopropyl ethyl acetal were synthesized according to published procedures.[7] THF, benzene, and ether were distilled from sodium−benzophenone. (Diphenylmethyl)potassium (Ph_2CHK) in tetrahydrofuran (THF) solution was synthesized according to well-established procedures. All the other materials were used as received.

Brij98 (Sigma) is a commercial emulsifier, poly(oxyethylene-(20)) oleyl ether, with molecular weight 1150. Potassium persulfate ($K_2S_2O_8$, Fluka) and sodium hydrogen carbonate ($NaHCO_3$, Merck), were used as initiator and buffer, respectively. Aerosol MA80 (sodium dihexyl sulfosuccinate, Cyanamid) was the surfactant in the polymerizations of the polystyrene seeds.

In the polymerization of the shells, potassium persulfate ($K_2S_2O_8$, Fluka) and disodium hydrogen phosphate (Na_2HPO_4, Panreac) and sodium dihydrogen phosphate monohydrate ($NaH_2PO_4 \cdot H_2O$, Merck) were used as initiator and buffers, respectively. In these copolymerizations the surfactant was sodium lauryl sulfate (SLS, Merck).

Doubly deionized water (DDI) was used throughout the work.

Methods. All anionic polymerizations were performed under an inert atmosphere using a reactor equipped with an argon inlet, magnetic stirring, sampling device, and burets meant to introduce solvent, monomer, etc.

NMR spectra were performed using a Bruker AC200 spectrometer.

Size exclusion chromatography was performed using a JASCO HPLC pump type 880-PU, TOSOHAAS TSK gel columns, a Varian series RI-3 refractive index detector, and a JASCO 875 UV/vis absorption detector with tetrahydrofuran as the mobile phase. Calibration was performed by means of polystyrene standards.

Emulsion polymerizations were carried out in a 1 L jacketed glass reactor fitted with a reflux condenser, stainless steel stirrer, sampling device, and nitrogen inlet tube.

I. Synthesis of ω-Styrene PEO Macromonomer 4 ($\bar{M}_n$ = 2010 Targeted). 3,3-Diethoxypropanol (**1**) (1.8 mL, 0.0114 mol) was dissolved in 200 of mL THF. A THF solution of (diphenylmethyl)potassium (25 mL, 0.0114 mol) was slowly added over a period of 1 h. The solution was then cooled to −30 °C, and ethylene oxide (22.8 mL, 0.456 mol) was added. The temperature of the solution was allowed to rise to room temperature, and the medium was further stirred for 48 h. Deactivation of the reaction medium was performed by addition of *p*-(chloromethyl)styrene (8.5 mL, 0.06 mol). The KCl salt formed was removed by filtration. The PEO macromonomer *(4)* was isolated by precipitation by ether.

Table 1. Polymerization Recipes of the Core Latexes[a]

	C1	C2
styrene wt (g)	262.970	263.160
aerosol MA80 wt (g)	11.470	8.500
$NaHCO_3$ wt (g)	1.000	1.000
$K_2S_2O_8$ wt (g)	1.007	1.000
H_2O wt (g)	624.970	625.010

[a] The reaction temperature in both reactions was 90 °C.

I.1. Transformation of the Macromonomer Acetal End Group into Aldehyde M1. A THF solution of PEO macromonomer **4** (0.66 g, 3.3×10^{-4} mol) was introduced to a flask equipped with a magnetic bar and containing 400 mL of acetone. Hydrochloric acid (0.5 mL, 6×10^{-3} mol) was slowly added to above the reaction medium, which was stirred for 1 h. After neutralization of the medium by K_2CO_3 and filtration, the PEO macromonomer M1 was removed by precipitation in ether.

II. Synthesis of PS-*b*-PEO Macromonomer M2. II.1. Synthesis of α-Acetal, ω-Styrene PS Macromonomer 8 ($\bar{M}_n$ = 2200 Targeted). In a typical reaction, styrene (23 mL, 0.2 mol) and TMEDA (3 mL, 0.02 mol) were dissolved in 250 mL of benzene at 15 °C. The above-described initiator **7** (20 mL, 1.2×10^{-3} mol) in solution in diethyl ether was added at once after filtration of lithium and the salts present. The reaction medium was then warmed to 25 °C and stirred for 2 h. 1,1-Diphenylethylene (7 mL, 0.04 mol) was first introduced to end-cap the PS chains with carbanions of lesser reactivity and the latter were then deactivated by addition of *p*-(chloromethyl)styrene (**3**) (8.5 mol, 0.06 mol). Precipitation by methanol yielded the expected macromonomer.

II.2. Transformation of the PS Macromonomer 8 Acetal End Group into Hydroxyl by Amberlyst Resin. A THF solution of the PS macromonomer **8** (5 g) was introduced into a 500 mL flask equipped with a magnetic stirring bar. Then, successively, acetone (375 mol), the Amberlyst resin (6 g), and some drops of water were added. After 12 h of stirring, the macromonomer was isolated after filtration of the resin and precipitated by methanol. After several freeze-dryings in dioxane, the macromonomer **9** was ready for the growth of the PEO block.

II.3. Growth of the PEO Block and Functionalization ($\bar{M}_{n,PEO}$ = 2000 Targeted) of M2. α-Hydroxyl, ω-styrene PS macromonomer **9** (5 g, 2.5×10^{-3} mol) was dissolved in 150 mL of THF. (Diphenylmethyl)potassium in THF solution was slowly added (5.4 mL, 2.5×10^{-3} mol). The solution was then cooled to 0 °C, and ethylene oxide (6 mL, 0.12 mol) was added. The temperature of the solution was allowed to rise to room temperature, and the medium was further stirred for 48 h. The alkoxides carried by the PEO blocks were deactivated using 2 mL (0.018 mol) of tresyl chloride. Twelve hours after addition of tresyl chloride, potassium 2,2-diethoxyethanolate (3.3 g, 2.5×10^{-3} mol), obtained by deprotonation using (diphenylmethyl)potassium, was introduced. After 24 h of stirring, the KCl salt formed was removed by filtration and macromonomer M2 was isolated by precipitation in pentane.

III. Emulsion Polymerizations. All of the core−shell type polymer particles were obtained by a two-step emulsion polymerization process. In the first step, the cores of the polymer particles (the seed used in the second step) were prepared at 90 °C by batch emulsion homopolymerization using the recipes given in Table 1. After polymerization, the seeds were kept overnight at 90 °C to decompose the initiator.

The seeded batch emulsion copolymerization of St and macromonomers was carried out to put the shell onto the polystyrene core synthesized in the first step, using the recipe given in Table 2. The reaction temperature was 70 °C in all shell reactions. The weight ratio of the comonomers was 9/1 (St/macromonomer) in all of the copolymerizations, except for the C2M2. The initiator concentration was 3.2% of the total monomer. The monomer/water ratio was maintained at 1/33.5.

Table 2. Polymerization Recipes of the Core−Shell Latexes[a]

	C1M1	C1M2	C1Brij	C2M1	C2M2	C2Brij
seed type	C1	C1	C1	C2	C2	C2
seed wt (g)	146.720	73.947	73.910	147.811	73.897	73.990
styrene wt (g)	10.758	5.467	5.471	10.863	5.430	5.434
macromonomer type	M1	M2	Brij98	M1	M2	Brij98
macromonomer wt (g)	1.225	0.595	0.601	1.204	0.563	0.601
SLS wt (g)	0.864	0.430	0.303	0.264	0.124	0.302
$K_2S_2O_8$ wt (g)	0.389	0.195	0.195	0.388	0.192	0.191
Na_2HPO_4 wt (g)	2.735	1.366	1.366	2.724	1.364	1.365
$NaH_2PO_4 \cdot H_2O$ wt (g)	4.428	2.213	2.212	4.428	2.212	2.217
H_2O wt (g)	402.651	201.011	201.500	402.942	201.644	201.400

[a] The reaction temperature in all the polymerizations was 70 °C.

The amounts of the buffers were calculated to obtain a final pH of approximately 6.6−6.8 and the emulsifier concentration in the case of C1M1, C2M1, C1M2, and C2M2 was calculated to cover 35% of the surface of the cores. In the case of polymerizations with Brij98, the amount of SLS was 5% of the total monomer weight used in the shell reactions.

Latexes C1M1, C1M2, and C1Brij were synthesized using the C1 seed, and for the latexes C2M1, C2M2, and C2Brij the seed was C2. The weight of polymer in the seed was 45 g (ca. 147 g of latex) in the cases of C1M1 and C2M1 and 22.5 g (ca. 74 g of latex) in the synthesis of C1M2, C1Brij, C2M2, and C2Brij latexes.

DDI water, buffer solution, and seed were charged into the reactor and purged with nitrogen for 20 min. Monomers were added, and the system was stirred and purged with N_2 at 30 °C to swell the seed particles with the comonomer. After 3 h, the temperature of reaction mixture was increased to 70 °C. Once the reaction temperature was reached, the aqueous solution of initiator was then added to the reaction mixture to start the polymerization. The stirring rate was 160 rpm, and the reaction time, 5 h. The final latex was left overnight at 70 °C to decompose the nonreacted initiator.

IV. Latex Characterizations. The overall conversions (x%) of the reactions at the end of the polymerizations were determined gravimetrically and the final pHs were measured.

Three methods were used for particle size determination: photon correlation spectroscopy (PCS, Coulter N4Plus), disk centrifuge (DCP, Brookhaven Instruments Corp.), and transmission electron microscopy (TEM, H7000 FA Hitachi).

The number (d_n) and weight (d_w) average diameters and the polydispersity index (PDI) were calculated from the particle size distribution (PSD).[8]

The amount of surface strong and weak acid groups was determined by conductometric titrations. The latexes were cleaned by means of a serum replacement cell before titration.

The conductometric titrations were carried out at 30 °C and the weight of the sample was 25 g with ca. 1.5% solid content. All the titrations were carried out at least twice.

The determination of the surface charge density (σ) was made by using the volume and concentration of the titration agent (NaOH) used, and the surface area of the latex particles.[9]

The electrokinetic behavior of the latexes was studied by measuring the electrophoretic mobility (μ_e) of the cleaned core−shell latexes in solutions of KBr of different concentrations and pHs.

The measurements of μ_e were carried out in the Grupo de Fisica de Fluidos y Biocoloides of the University of Granada, using a Malvern ZetaSizer4.

V. Colloidal Stability. The colloidal stability was determined in terms of critical coagulation concentration (CCC), following the coagulation kinetics using the turbidimetric method.[10,11]

The kinetics of coagulation were measured using a spectrophotometer (Spectronic Genesys5, Milton Roy) at 550 nm, and different concentrations of a KBr solution were used.

The concentrations of the samples were chosen to have an initial absorbance of 0.4−0.6, which corresponds to ca. 5×10^{11} particles/mL for the latexes with the core C1 and ca. 3×10^{10} particles/mL for the latexes with the C2 core. The pH of latexes was adjusted to the required values using 0.025 M NaOH or 0.1 M HCl. Buffers with low ionic strength were tried too, but the pHs measured did not correspond to those expected ones. The buffers' capacities were not high enough.

The kinetics of coagulation were measured for 30 s after mixing the latex and electrolyte (ratio 4/1) in the spectrophotometric cell.

VI. Hairy Layer on the Particle Surface (Spacers). The surface of latex particles is very often coated with a layer of surface active material (spacers), which can be physically adsorbed or covalently bound. Their concentration profile will be distance-dependent and the distribution of the segments on the surface, e.g., in loops, trains, and tails, will not be homogeneous; i.e., the "bare surface" of the native particle becomes "hairy". The adsorbed layer modifies the particle−particle interactions. This hairy layer structure is often responsible for the enhanced stability of the polymers (steric stabilization), but complete coverage of the particle surface is required. Otherwise, the adsorbed surface active molecules can induce instability in the disperse system (bridging).[12]

The solvent power of the dispersion medium for the stabilizing spacers is another important item. With the decreasing solvent power of the medium, the stability of the particles decreases. In our case, the stabilizing moiety is PEO. Above a certain concentration of a 1:1 electrolyte, the solution becomes a poor solvent for PEO;[13] thereby, one can expect the spacers to collapse onto the particle surface and the steric stabilizing effect to vanish.

On the other hand, the dependence of the hairy layer thickness on the electrolyte concentration can be used to determine the length of the spacers, using the PCS technique for example (see later).

Another possibility to determine the hairy layer thickness, is to measure the diameter of the particles with DCP at different disk speeds, supposing that at low disk speed the spacers straighten out into the water phase, while at high disk speed they are collapsed to the surface.

VII. Adsorption of Macromonomers to the Surface of Core Latexes. To determine the saturation concentration of adsorption of macromonomers into the cores (C1, C2), surface tension measurements were carried out with M1 and Brij98. The equipment used for these experiments was a KSV Sigma 70 (KSV Instruments Ltd.) tensiometer.

M1 and Brij98 contain both hydrophilic and hydrophobic parts; hence, the presence of these materials in a solution decreases its surface tension.

In our case, polystyrene particles are also present in the solution and the surface active material before micelle formation has to saturate the surface of polystyrene particles, too. If the solubility of surfactant in the aqueous phase is low and considering that the liquid−gas interphase is negligible in comparison with the latex particle surface, the critial micelle concentration (CMC) can be used to estimate the saturation concentration at the surface of the latex particles.[14]

The surface tension measurements were carried out in the following way. A set of solutions with a constant amount of cleaned core latex and varying amounts of macromonomer solutions were mixed. The solutions were left at least 12 h to reach equilibrium, and their surface tensions were measured.

Results and Discussion

I. Synthesis of α-Functionalized, ω-Unsaturated PS/PEO Macromonomers. For the proposed application, the macromonomers should be constituted of a hydrophobic head—the latter fitted with an unsaturation that will subsequently serve to anchor the macromonomer to the latex particle—and of an acetal or aldehyde tail to enable the reaction of particles formed with the amino group of biomolecules.

Two families of PEO macromonomers have been prepared:

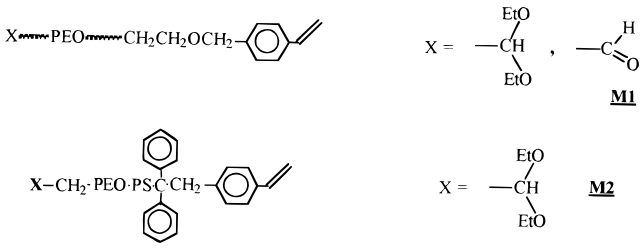

In the first family, the hydrophobic head only consists of an end-standing styrene unsaturation, whereas, in the second family, a genuine PS block fitted with a styrenic unsaturation serves as the hydrophobic part.

The nature of the functional group and the respective size of the hydrophobic and hydrophilic blocks are two parameters that can modify the characteristics of the particles formed after the grafting of these macromonomers.

To obtain these macromonomers, we resorted to "living" anionic polymerization and to the end functionalization of living anionic species. Macromonomers with a narrow distribution of molecular weights and high functionalization yield can be obtained in this way. Out of the two pathways that can be followed to introduce the polymerizable group at the macromonomer chain end,[15] we chose to use that based on the deactivation of growing sites.

I.1. Synthesis of α-Aldehyde, ω-Styrene PEO Macromonomers M1. I.1.1. Synthesis of α-Acetal, ω-Styrene PEO Macromonomers (4). PEO macromonomers, bearing an acetal function in the α position and a styrenic unsaturation in the ω position, were obtained in a one-pot synthesis.

A potassium alkoxide ***(2)*** containing an acetal group was used as initiator of the polymerization of ethylene oxide, which was carried out in THF.

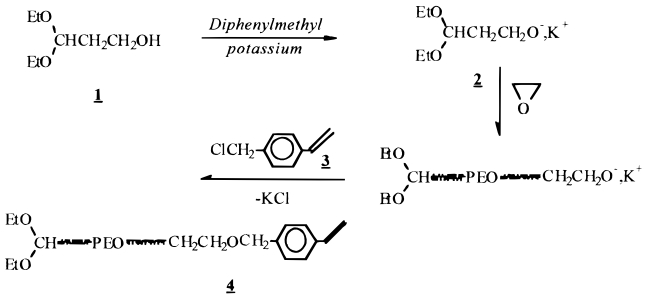

The deprotonation of **1** by (diphenylmethyl)potassium must be effected with great care: any excess of this deprotonating agent can indeed give rise to unfunctionalized chains. As for the unsaturation, it was introduced through deactivation of the growing alkoxides by *p*-(chloromethyl)styrene (**3**).

Table 3. Characteristics of α-Acetal, ω-Styrene PEO Macromonomers

$\bar{M}_{n,macro}$ (targeted)	$\bar{M}_{n,macro}$[a] (^{1}H NMR)	$\bar{M}_w/\bar{M}_n$[b] (SEC)	f[c]
2010 (M1)	2000	1.06	0.94
2010	1850	1.08	0.90
2010	2150	1.08	0.80
2010	1550	1.07	0.93

[a] $\bar{M}_{n,macro} = 44\,(I_3/4I_1) + 220$; I_1 and I_3 are the intensities of the signals due to the acetal proton ($\delta = 4.6$ ppm) and to CH_2O protons ($\delta = 3.3-3.7$ ppm). [b] Calibration by linear PS standards. [c] $f = I_2/3I_1$; I_1 and I_2 are the intensities of the signals due to the acetal proton ($\delta = 4.6$ ppm) and to ethylenic protons of styrene ($\delta = 5.2-6.7$ ppm), respectively.

Scheme 1

^{1}H NMR.

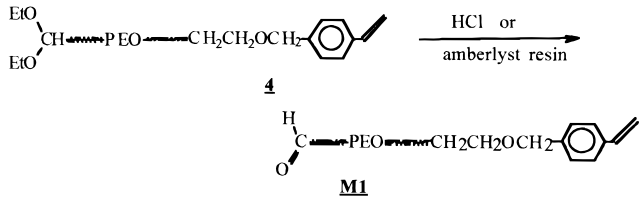

Table 4. Transformation of the Acetal Group into an Aldehyde

reacn time (h)	10^5[HCl] (mol/L)	conversion[a] (%)
5	3.2	70
1	1.5	96

[a] It is equal to $(3I_3/I_2)100$; I_2 and I_3 are the intensities of the signals due to the ethylenic protons of styrene ($\delta = 5.2-6.7$ ppm) and to the aldehyde proton ($\delta = 9.7$ ppm), respectively.

The data pertaining to the four macromonomers synthesized by this method are given in Table 3; only M1 has been subsequently used for the latex particle synthesis. The samples were characterized by ^{1}H NMR (Table 3) and SEC. All macromonomers **4** exhibit polydispersity indexes close to unity; their $\bar{M}_n$'s, determined by SEC and cross-checked by NMR upon comparing the peak due to their acetal functionality with that arising from the ethylene oxide units, are found in good agreement with the targeted values. The extent of functionalization by (chloromethyl)styrene (**3**) was also checked by ^{1}H NMR through the comparison of the signal due to the proton of the acetal function ($\delta = 4.6$ ppm) with that arising from the ethylenic protons of the styryl moiety ($\delta = 5.2-6.7$ ppm). Polymers with functionalities close to the targeted values were systematically obtained, indicating that initiation by **2** occurred as expected and deactivation by **3** was selective.

I.1.2. Transformation of the Macromonomer Acetal End Group into Aldehyde M1. The transformation of the acetal function into an aldehyde end group was effected using hydrochloric acid (Scheme 1). The extent of the chain end modification was checked by ^{1}H NMR. The reaction was carried out for various reaction times and at two hydrochloric acid concentrations (Table 4). The best results (96% conversion) were obtained at low acid concentration and with short reaction times (Figure 1). In this case the SEC chromatograms of the ω-acetal **4** and ω-aldehyde macromonomers M1 are the same. Macromonomers obtained after longer reaction times or with higher acid concentrations exhibit a bimodal distribution. A peak of small size appears at a retention volume corresponding to

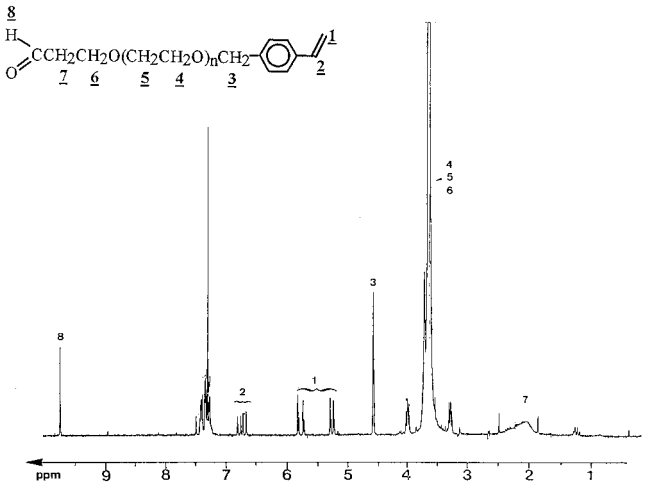

Figure 1. ^{1}H NMR spectrum ($CDCl_3$) of α-aldehyde, ω-styrene PEO macromonomer (M1).

twice the molecular weight attributed to the major peak. This feature might be due to the aldol condensation that is known to occur in acidic medium.[16]

Previously, Scholz et al. reported a similar side reaction while attempting to transform acetals into aldehyde groups on the surface of a polymeric micelle.[17]

I.2. Synthesis of α-Aldehyde, ω-Styrene PEO-*b*-PS Macromonomer M2. The PEO macromonomer described in the above section was fitted with a hydrophobic styrenic head. To get access to macromonomers with a larger hydrophobic part but similar styrenic head and acetal tail, we designed an original two-step synthesis, the one-pot strategy used above being not appropriate for this kind of macromonomer.

As for the two PS and PEO blocks, they were obtained by living anionic polymerizations of styrene and oxirane.

I.2.1. Synthesis of α-Acetal, ω-Styrene PS Macromonomer (8). The first step consisted of the preparation of an α-hydroxyl, ω-styrene PS macromonomer. The hydroxyl function present in the α position was used in a second step to grow the PEO block, the latter being subsequently end-fitted with an acetal group function. The aldehyde function that is required for the envisaged biomedical application was derived by the same method as that described above.

Table 5. Characteristics of PS and PS-*b*-PEO Macromonomers

	$\bar{M}_n$ (targeted)	$\bar{M}_{n,PEO}$[a] (NMR)	$\bar{M}_{nPS}$ (NMR)	$\bar{M}_{nPS}$ (SEC)	$\bar{M}_w/\bar{M}_n$ (SEC)	f[b]	g[c]
PS	2010		2000	1950	1.09	0.93	
PS−PEO[d]	4000	1785	2000		1.05		0
PS−PEO[e]	4000	3550	2000		bimodal		0.78
PS	2010		2400	2350	1.11	0.95	
PS−PEO[f] (M2)	4200	2000	2400		1.80		0.96

[a] $\bar{M}_{n,PEO} = 44(3I_3/4I_2)$. [b] $f = I_2/3I_1$; I_1 and I_2 are the intensities of the signals due to the acetal proton ($\delta = 4.6$ ppm) of 3-chloro-1,1-diethoxypropane and to ethylenic protons of styrene ($\delta = 5.2-6.7$ ppm), respectively. [c] $g = 4I_1/I_2$; I_1 and I_2 are the intensities of the signals due to the acetal proton of (2,2-diethoxyethanol) ($\delta = 4.6$ ppm) and to protons of styrene end group ($\delta = 5-6.1$ ppm), respectively. [d] Deactivation by 2-chloro-1,1-diethoxyethane. [e] Deactivation with only 2 equiv of tresyl chloride. [f] Deactivation with 7 equiv of tresyl chloride.

Scheme 3

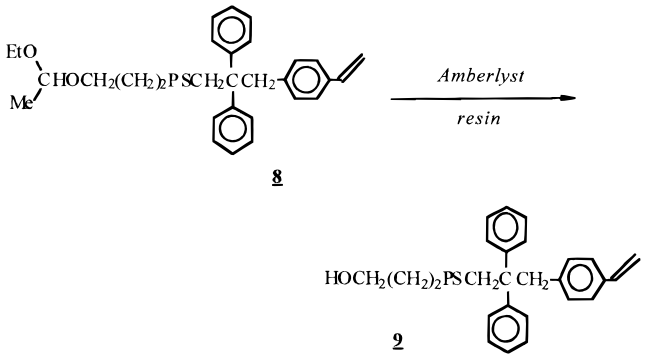

PS living chains were first prepared using the lithiated initiator **7** that also possesses an acetal group (Scheme 2). The method followed to generate **7** from **6** was previously described.[7] After polymerization of styrene, the styryl carbanions were then end-capped with 1,1-diphenylethylene, a step that gave rise to carbanions of moderate and suitable reactivity for the deactivation by *p*-(chloromethyl)styrene (**3**). The acetal group that is introduced with the initiator moiety was purposely chosen to give rise to an end-standing hydroxyl function upon cleavage in acidic medium. This hydroxyl can indeed be subsequently used to grow the

Scheme 2

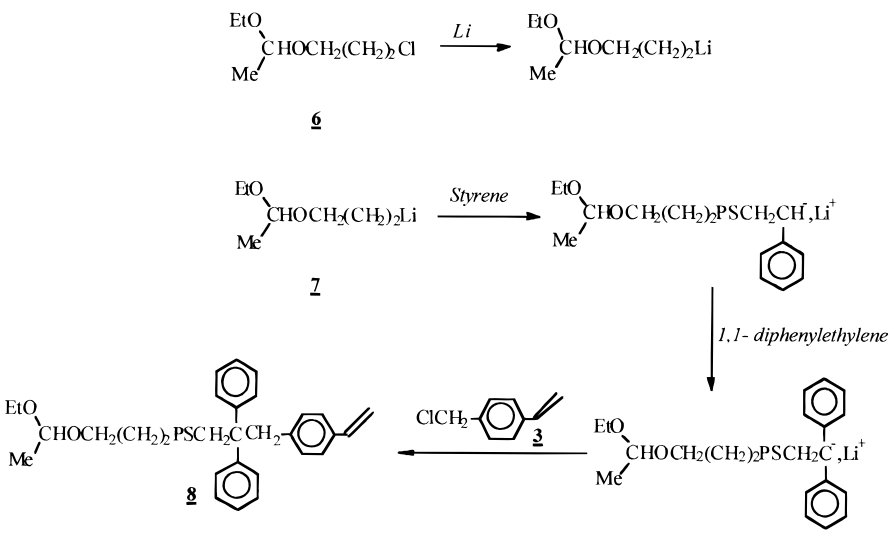

Scheme 4

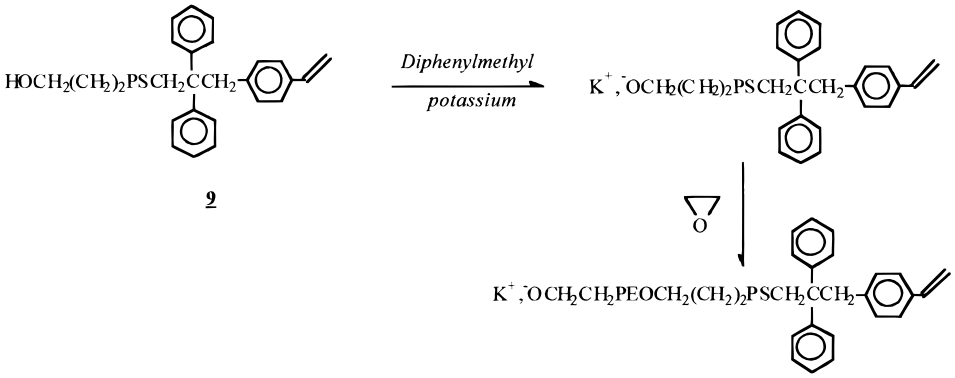

Scheme 5

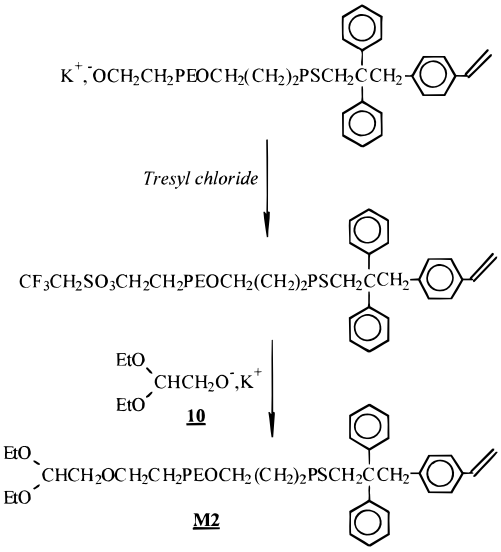

Scheme 6

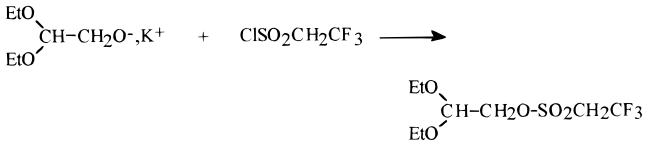

PEO block after deprotonation by (diphenylmethyl)-potassium.

The PS macromonomers ***8*** obtained were recovered by precipitation using methanol and analyzed by SEC (Table 5); they were found to exhibit polydispersity indexes close to unity and molecular weight in good agreement with the expected values. The functionalization of these macromonomers that was checked by ^{1}H NMR was found to be quantitative.

I.2.2. Cleavage of the Acetal Group. The transformation of the acetal function carried by **8** into an hydroxyl group (Scheme 3) was achieved using the Amberlyst resin and appeared to be straightforward: the yield of the reaction was indeed quantitative.

I.2.3. Growth of the PEO Block and Acetal Functionalization. The ω-hydroxyl PS macromonomer **9**, obtained previously, was deprotonated by (diphenylmethyl)potassium, following the same pathway (Scheme 1) as that used for the synthesis of PEO macromonomer (M1), and the alkoxides formed were then used to grow the PEO block, as shown in Scheme 4.

The introduction of the acetal group was effected during the deactivation step. Attempts to deactivate the growing potassium alkoxides by a chloro compound such as 2-chloro-1,1-diethoxyethane proved to be unsuccessful because of their little mutual reactivity. Another pathway was thus envisaged: the growing alkoxide species were first deactivated by an excess of tresyl chloride (Scheme 5); the electrophilic tresylate functions introduced in this way were further reacted with **10**, which is a potassium alkoxide possessing an acetal group (Scheme 5). Tresyl chloride being used in excess to make sure that all PEO block ends are fitted with tresylate functions, a 3-fold excess of **10** as compared with the amount of tresyl chloride had to be introduced in the reaction medium: **10** can indeed react with residual tresyl chloride (Scheme 6), besides the condensation on the tresylate carried by the macromonomer.

The α-acetal, ω-styrene PEO-*b*-PS macromonomer M2 was isolated by precipitation in pentane and characterized by ^{1}H NMR (Figure 2) and SEC. The SEC analysis before and after the growth of the PEO block indicates that all PS chains actually initiated the polymerization of ethylene oxide. As for the chain end functionalization, it was found to be quantitative (Table 5) according to NMR characterization.

II. Characterization and Colloidal Properties of the Latex Particles. In Table 6, the overall conversions (x%) of the cores and core−shell latexes, the solid content (%), and the final pHs are shown. The overall conversions were in all cases, except C1M2, almost 100% within experimental error. The final pHs were practically neutral.

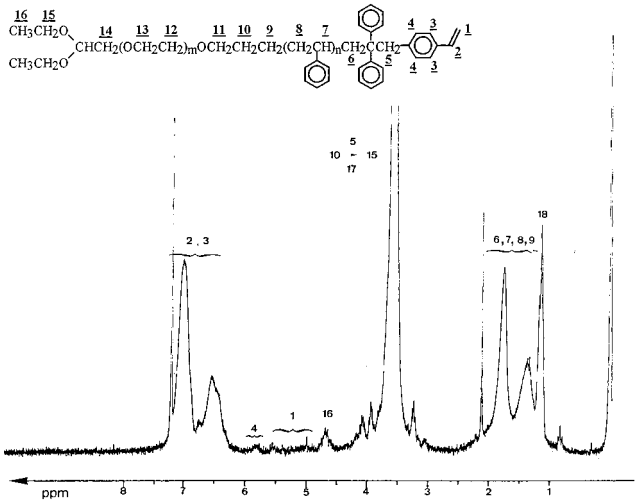

Figure 2. ^{1}H NMR spectrum ($CDCl_3$) of the PS-*b*-PEO macromonomer *M2* fitted with acetal and styrene end groups in the α and ω positions, respectively.

Table 6. Overall Conversions (*x*%), Solid Contents, and Final pHs of the Latexes

latex	*x*%	solid content (%)	final pH
C1	98.4	30.67	7.8
C2	99.7	30.45	7.7
C1M1	97.8	11.50	6.5
C1M2	75.0	9.70	6.6
C1Brij	92.8	9.22	6.5
C2M1	98.5	11.40	6.4
C2M2	97.4	11.24	6.4
C2Brij	100.0	11.32	6.5

Table 7. Particle Sizes and PDIs of the Latexes

		TEM			DCP		
latex	PCS d (nm)	d_n (nm)	d_w (nm)	PDI	d_n (nm)	d_w (nm)	PDI
C1	119.8	103.9	105.4	1.014	118	132	1.119
C2	186.8	161.2	163.6	1.015	195	219	1.123
C1M1	151.0	109.6	116.4	1.063	136	172	1.265
C1M2	147.0	111.8	114.7	1.025	131.5	138	1.049
C1Brij	136.9	122.2	124.2	1.017	130.5	139	1.065
C2M1	233.9	185.5	196.4	1.059	232	282	1.22
C2M2	214.4	188.2	194.6	1.034	206	222	1.080
C2Brij	209.4	191.0	193.6	1.011	219	241	1.100

Table 7 presents the particle sizes and PDIs of the synthesized latexes, as measured by PCS, TEM, and DCP: The results showed that the latexes could be considered monodisperse (according to TEM).[18]

In Table 8, the amounts of surface strong and weak acid groups and the surface charge densities (σ) are shown. The low contents of strong acid groups (sulfate groups) provided by the initiator and weak acid groups (carboxylic groups) provided by the macromonomers are the cause of the low surface charge densities of the core−shell latexes. The increase in the total surface charge densities of the core−shell latex particles, compared to the cores, were mainly due to the weak acid groups provided by the macromonomers.

The surface sulfate groups (strong acid) are produced due to the cleavage of the initiator as sulfate anion radicals:

$$S_2O_8^{2-} \rightarrow 2\ {}^{\bullet}SO_4^-$$

$$^{\bullet}SO_4^- + n\ CH_2{=}CH \rightarrow {}^{\bullet}(CH_2\text{-}CH)_n\text{-}SO_4^-$$
$$\qquad\qquad\qquad\qquad\quad |\qquad\quad |$$
$$\qquad\qquad\qquad\qquad C_6H_5 \quad C_6H_5$$

Several possible sources can be responsible for the formation of carboxylic (weak acid) groups: hydrolysis of sulfate groups followed by oxidation, dissolution of carbon dioxide in the latex, oxidation of surface sulfate groups—particularly in the presence of small concentrations of heavy metal ions—side reactions of initiating species,[19] and/or partial oxidation of the macromonomers M1 and M2. Aldehydes and even acetal are indeed fragile groups that can be easily transformed into carboxylic acids.[9]

The results of the electrophoretic mobility (μ_e) measurements of the cleaned C1M1, C1M2, and C2M2 latexes at different ionic strengths and pHs with the estimated diameters (d_p), are shown in Tables 9 and 10. The electrophoretic mobility varied with ionic strength and pH similarly for all latexes. Above 0.01 M of electrolyte (log $C_{KBr} \geq -2$) and below pH = 6, the decrease in μ_e was significant. The electrophoretic mobilities in all cases were negative, arising from the acid groups. The decrease at low pH (and high KBr concentration) can be assigned to neutralization of strong acid groups (at pH 4.5−5.5, determined by

Table 8. Amounts of Surface Groups and Total Surface Charge Densities (σ_{total}) of the Latexes

	strong acid			weak acid			
latex	mmol/g	mmol/cm^2	σ_{strong} (μC/cm^2)	mmol/g	mmol/cm^2	σ_{weak} (μC/cm^2)	σ_{total} (μC/cm^2)
C1	1.40×10^{-3}	0.27×10^{-8}	0.25				0.25
C2	3.94×10^{-3}	1.44×10^{-8}	1.38				1.38
C1M1	1.54×10^{-3}	0.35×10^{-8}	0.34	2.80×10^{-3}	0.65×10^{-8}	0.62	0.96
C1M2	3.62×10^{-3}	0.85×10^{-8}	0.82	4.21×10^{-3}	$0.99 \times 10^{--8}$	0.95	1.77
C1Brij	1.99×10^{-3}	0.43×10^{-8}	0.42	10.64×10^{-3}	2.31×10^{-8}	2.23	2.65
C2M1	6.50×10^{-3}	2.61×10^{-8}	2.51	4.70×10^{-3}	1.88×10^{-8}	1.82	4.33
C2M2	2.24×10^{-3}	0.77×10^{-8}	0.74				0.74
C2Brij	3.61×10^{-3}	1.17×10^{-8}	1.13	5.03×10^{-3}	1.63×10^{-8}	1.57	2.70

Table 9. Electrophoretic Mobilities (μ_e) and Estimated Diameters (d_p) for KBr Solutions of Different Ionic Strengths

	C1M2		C1M1		C2M2	
log C_{KBr}	$10^8\mu_e$ (m^2/Vs)	d_p (nm)	$10^8\mu_e$ (m^2/Vs)	d_p (nm)	$10^8\mu_e$ (m^2/Vs)	d_p (nm)
−4.0	−3.728 ± 0.075	136	−4.203 ± 0.100	135	−4.003 ± 0.035	166
−3.5	−3.677 ± 0.065	133	−4.006 ± 0.065	137	−3.976 ± 0.075	162
−3.0	−3.955 ± 0.050	127	−4.517 ± 0.080		−4.423 ± 0.100	152
−2.5	−4.110 ± 0.080	137	−4.524 ± 0.150	139	−4.780 ± 0.100	151
−2.0	−3.680 ± 0.070	131	−4.246 ± 0.160	136	−4.421 ± 0.060	163
−1.5	−2.765 ± 0.050	124	−3.254 ± 0.170	147	−3.408 ± 0.075	165
−1.0	−1.842 ± 0.150	149	−2.110 ± 0.120	190	−2.436 ± 0.070	191

Table 10. Electrophoretic Mobilities (μ_e) and Estimated Diameters (d_p) for Different pHs

	C1M2		C1M1		C2M2	
pH	$10^8\mu_e$ (m^2/Vs)	d_p (nm)	$10^8\mu_e$ (m^2/Vs)	d_p (nm)	$10^8\mu_e$ (m^2/Vs)	d_p (nm)
4	−0.742 ± 0.030	229	−0.690 ± 0.030	309	−0.628 ± 0.035	438
5	−2.540 ± 0.046	146	−1.606 ± 0.080	204	−1.606 ± 0.140	228
6	−3.978 ± 0.065	131	−4.607 ± 0.095	169	−4.521 ± 0.040	196
7	−4.111 ± 0.115	136	−4.711 ± 0.090	162	−4.552 ± 0.080	198
8	−3.804 ± 0.080	137	−4.325 ± 0.090	165	−4.253 ± 0.070	201
9	−3.999 ± 0.061	135	−4.675 ± 0.095	165	−4.297 ± 0.120	202
10	−4.077 ± 0.077	135	−4.367 ± 0.050	166	−4.520 ± 0.045	200

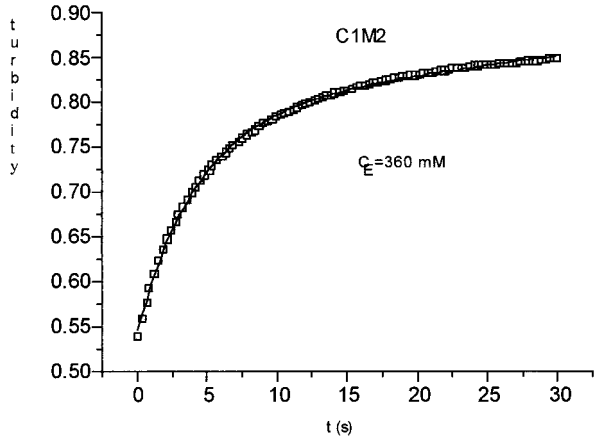

Figure 3. Evolution of the turbidity during the fast coagulation of C1M2: (□) experimental values; (—) curve fit. The concentration of electrolyte was 360 mM.

potentiometric titrations). The variation in the basic region (pH > 7−10) is not significant, despite the presence of a significant amount of weak acid groups, whose protonation process takes place at pH 7−8 (determined by potentiometric titration). This process has practically no effect on the electrophoretic mobility.

In the cases of C2M2 and C1M2, the diameter varied with ionic strength, while in the case of C1M1, the differences were negligible. In all cases, at high electrolyte concentrations, significant increases in the average diameter can be observed, due to the coagulation of particles. The same results were found at low pHs.

To evaluate the critical coagulation concentration (CCC) of the latexes, the coagulation kinetics (turbidity vs time) of the latexes were measured. After that, the experimental curves were fitted by the following function (Figure 3):

$$\tau = A_0 - C_1 e^{-C_2 t} + A_1 t \qquad (1)$$

where A_0, A_1, C_1, and C_2, are constants and the fitted parameters are τ, turbidity, and t, time.

The reaction rate of the process was determined as the time derivative of the theoretical curve:

$$\frac{d\tau}{dt} = C_2 C_1 e^{-C_2 t} + A_1 \qquad (2a)$$

The initial rate of the coagulation process can be obtained by substituting 0 for t:

$$\frac{d\tau}{dt}(0) = C_2 C_1 + A_1 \qquad (3)$$

If the electrolyte concentration is below the CCC (slow coagulation), the measured data can be fitted without the linear part ($A_1 t$) of eq 1, similarly to the first ca. 8−10 s of the fast coagulation process. This means that the fast coagulation process is initially governed by the exponential part of the equation, and the linear part only becomes significant later.

Substituting from (1) for the exponential term in eq 2a we obtain the equivalent form:

$$\frac{d\tau}{dt} = C_2[A_0 - \tau] + A_1(1 + C_2 t) \qquad (2b)$$

The first term indicates that the turbidity will exponentially approach the maximum value (of the exponential term) A_0, which might be the turbidity when all the particles are coupled to dimers. The linear term might be the linear term of the Taylor series of a second exponential term, expressing the turbidity of aggregates higher than dimers. The formation of higher aggregates during the measured time is limited, so its exponential law can be approximated by a linear one. The limiting value of the linear term for infinite time is also infinite, which is impossible for physical reasons. On the other hand, an exponential term (similar to the term in eq 1) has an upper asymptotic limit value. This means that the turbidity will not increase without limit, which is more acceptable behavior. According to this, we suggest that the whole coagulation, including not only dimers of particles but also bigger aggregates, can be expressed by a series of exponential terms, each of them assigned to one level of aggregation.

Table 11. Critical Coagulation Concentrations of the Synthesized Latexes and Corresponding Total Surface Charge Densities (σ_{total})

	pH = 7	pH = 2	σ_{total} (μC/cm^2)
C1	183.7	154.5	0.25
C2	259.9	254.8	1.38
C1M1	223.8	139.3	0.96
C1M2	169	151.1	1.77
C1Brij	179.5	139	2.65
C2M1	250	202	4.33
C2M2	264.5	251.6	0.74
C2Brij	264.5	184.7	2.70

Although the agreement between the theoretical and experimental curves is convincing (Figure 3), we admit that further investigation would be useful to test the above-mentioned hypothesis. However, this is outside the scope of this paper.

In Table 11, the CCCs of the latexes are shown. At pH = 7 it was ca. 250−265 for the C2 set of polymerizations, and 170−184 for the C1 set. The only exception was C1M1, with 223.8 mM. At pH = 2, the values were less than those at pH = 7, because of the protonation of surface groups. The CCCs of the core−shell latexes did not differ significantly from the CCCs of the cores. Although it was not possible to find a direct correlation between the surface charge and the CCC, the moderately low CCCs measured corresponded to the rather low surface charges of these latexes. The presence of polymeric chains on the particles surface (spacers) did not seem to have any effect on the colloidal stability of the core−shell latexes synthesized. To confirm the existence of these spacers on the surface, the determination of their length was carried out.

Due to the amphiphilic character of the macromonomer used in the shell reactions, it was most likely that the comonomer molecules were preferably located on the interphase between the latex and water phase and connected to the latex particles by their hydrophobic (styrene, polystyrene, or oleic acid) parts, whereas their hydrophilic (poly(ethylene oxide)) parts are expected to create the hairy layer of the latex particles.

To determine the thickness of the hairy layer (the length of the spacers), we used the DCP technique, assuming that at high disk speed the spacers were more or less compressed, while at low disk speeds they were straightened out. Comparing the two values, we could estimate the length of the spacers. Figures 4 and 5 show the dependencies of the particle size on the disk speed. The differences of the diameters for cleaned core−shell latexes measured at high and low disk speed

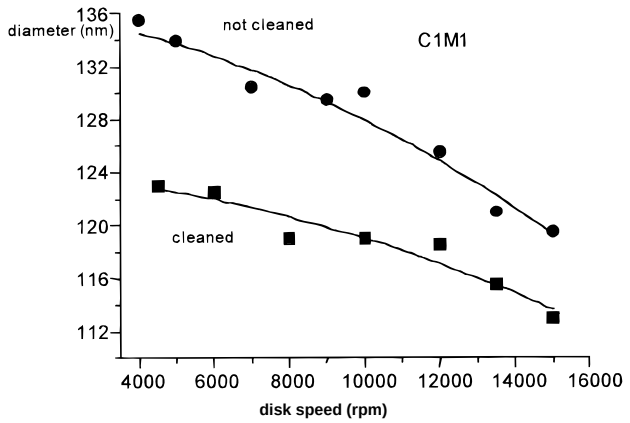

Figure 4. Particle diameter vs disk speed of the cleaned and uncleaned C1M1 latex measured by DCP.

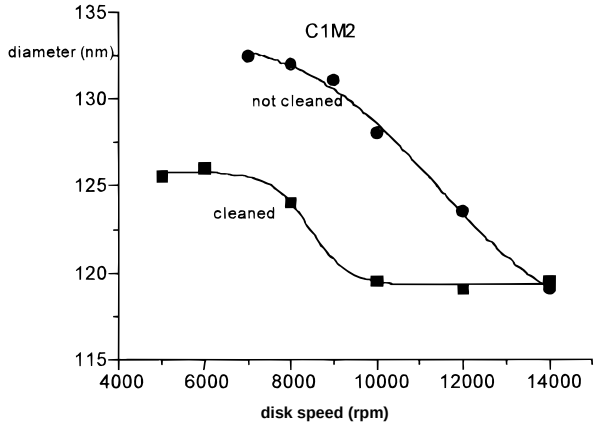

Figure 5. Particle diameter vs disk speed of the cleaned and uncleaned C1M2 latex measured by DCP.

were 7−9 nm, suggesting that the hairy layer thickness was 3.5−4.5 nm. The only exception was the latex C2M2, whose hairy layer thickness was 8 nm.

It was found that the diameters were different for cleaned and uncleaned latexes. The differences might be due to the desorption of only physically adsorbed macromonomer during the cleaning process. Usually with increasing disk speed these differences decreased, which means that, at high disk speeds, the latex particles lose the physically adsorbed molecules. Analyzing the near-UV spectra of the serum, from the serum replacement and the supernatant from ultrafiltration of latexes, confirmed the presence of macromonomers in the serum and supernatant.

Other means of determining the hairy layer thickness were the particle size and electrophoretic mobility in electrolytes of different ionic strengths. At high ionic strength the spacers were collapsed, due to the compression of the electrical double layer.

The influence of ionic strength on the spacers' length was investigated for C1M1, C2M1, and C1M2 latexes with PCS (Table 12). The decrease in the diameter was 7−9 nm, corresponding to a spacer length of 3.5−4.5 nm. At the highest concentration of KBr, the diameters increased, because of the beginning of the coagulation of the particles, similarly to electrophoretic mobility measurements (Table 9).

Furthermore, the increasing concentration of KBr in the solutions, used in the CCC experiments probably meant that, above a certain concentration, the KBr solution was a worse solvent than the Θ-solvent[13] for

Table 12. Diameters (±1 nm) of Latexes Measured by PCS at Different KBr Molar Concentrations

log C_{KBr}	C1M1	C2M1	C1M2
−6.0	147	231	139
−5.0	146	228	138
−4.0	144	228	137
−3.0	139	226	132
−2.0	139	224	132
−1.0	150	230	135

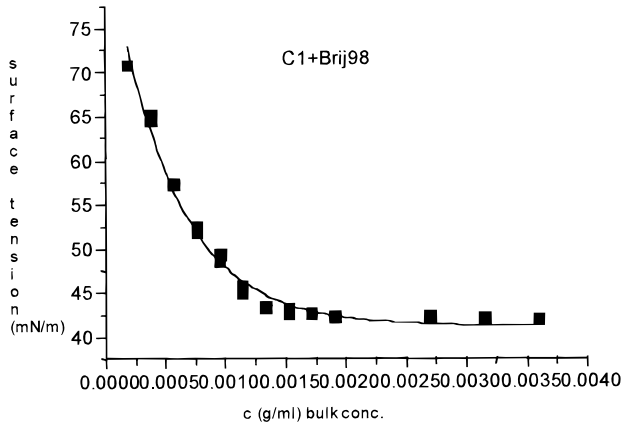

Figure 6. Surface tension vs bulk concentration of Brij98 on core C1.

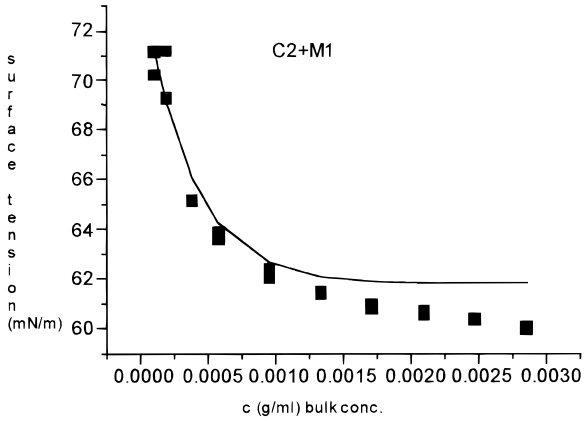

Figure 7. Surface tension vs bulk concentration of macromonomer M1 on core C2: (■) experimental values; (—) theoretical exponential decay.

poly(ethylene oxide) and the spacers collapsed onto the particle surface. The results of spacer length measured by PCS in KBr solutions of different concentrations (Table 12) and also the electrophoretic measurements (Table 9) seemed to support this hypothesis.

To estimate the surface coverage of the cores by the macromonomers and Brij98, during the core−shell reactions, the adsorption isotherms were determined, using surface tension measurements. Brij98 and M1 were used during these experiments. In Figure 6, the surface tension vs bulk concentration of Brij98 on the core C1 are shown. In the case of Brij98 the plot of surface tension vs bulk concentration of surfactant ($\gamma-C$) were the expected monoexponential decays, and the $\gamma-\log C$ was sigmoidal. In Figures 7 and 8, the surface tension vs bulk concentration of M1 ($\gamma-C$) on the core C2 and the $\gamma-\log C$ are shown, respectively. In the case of M1 the $\gamma-C$ curve was decreasing linearly at high concentrations instead of achieving a constant limiting value. Due to that, the $\gamma-\log C$ curve was not the expected sigmoidal. Decomposing the $\gamma-C$ curve to an exponential and a linear decay, from the exponential

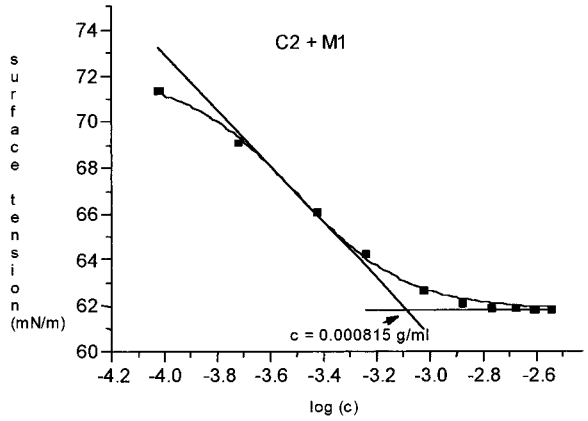

Figure 8. Determination of the CMC of M1 on the C2 core from the exponential part of Figure 7. The arrow shows the CMC.

part, it was possible to obtain the critical micelle concentration (CMC).

During the evaluation of the measurements, nonlinear regression was used. The equation fitted in the case of M1 macromonomer was

$$\gamma = P_1 + P_2 e^{-P_3 C} + P_4 C \tag{4}$$

where P_i are the parameters fitted and C is the bulk concentration of the macromonomer. By omitting the linear term (P_4C) and plotting γ vs log C, we obtained a sigmoidal curve. The function fitted to this curve was the Boltzmann equation:

$$\gamma = \frac{A_1 - A_2}{1 + e^{(x - x_0)/dx}} + A_2 \tag{5}$$

where A_1 and A_2 are the upper and lower limit values, respectively, x is the logarithm of bulk concentration of the surface active material, x_0 is the position of the inflection point ($\gamma = (A_1 + A_2)/2$), and dx determines the "width" of the curve. The CMC was determined from the intersection of the lower limit

$$\lim_{C \to \infty} \gamma = A_2 \tag{6}$$

and of the tangent at the inflection point

$$y = -\frac{A_1 - A_2}{4dx}(x - x_0) + \frac{A_1 + A_2}{2} \tag{7}$$

The intersection is at

$$x = x_0 + 2dx$$

or

$$\log C_{CMC} = \log C_0 + 2dx \tag{8}$$

This concentration was taken as the CMC and as the estimation of surface saturation concentration.

The unexpected behavior of M1 can be explained due to its higher solubility comparing with Brij98, which was visible during the experiments.

One of the requirements to determine the saturation concentration as mentioned above is the low surfactant solubility. In the case of M1 this requirement was not fulfilled. However, eliminating the linear part of the curve, arising from the solubility of M1, the break on the γ − log C curve could be assigned to the saturation of liquid−air and liquid−particle interphases.

Table 13. CMCs of M1 and Brij98 in the Presence of Cores C1 and C2

	C1 + Brij	C2 + Brij	C1 + M1	C2 + M1
CMC (g/mL) bulk solution	0.001 23	0.001 21	0.000 78	0.000 815
CMC (g/g) macromonomer/polymer	0.0858	0.0513	0.0544	0.0346
parking area (Å^2/molecule)	116	102	319	263

Table 14. Surface of the Cores and the Surface That the Surfactants Were Able to Cover[a]

polymerization of the core−shell latexes	C1M1	C1Brij	C2M1	C2Brij
core (cm^2)	2.35×10^7	1.25×10^7	1.36×10^7	6.82×10^6
MA80 (cm^2)	3.22×10^6	1.61×10^6	2.41×10^6	1.21×10^6
SLS (cm^2)	1.05×10^7	3.68×10^6	3.21×10^6	3.67×10^6
macromonomer (cm^2)	1.07×10^7	3.43×10^6	1.053×10^7	3.43×10^6
% of coverage	104	70	119	122

[a] The "% of coverage" was the ratio (in %) of the surfactant's equivalent surface and the surface of the core.

The results were compiled in Table 13, where the CMCs of M1 and Brij98 are presented, according to their bulk concentration in the solution and according to the amount of polymer in the latex added to these solutions. Finally, from the macromonomer/polymer ratio, the parking areas (the particle surface area occupied by one molecule of surfactant or macromonomer) were determined. The surface average diameters used in calculations were 109 nm for C1 and 208 nm for C2, determined by DCP at low disk speeds. For n-$C_{16}H_{33}$-$(-OC_2H_4)_{21}-OH$, which is comparable to Brij98, Elworthy[14] found a parking area of 120 Å^2/molecule. The values determined by us for Brij98 (102−116 Å^2/molecule) were in very good agreement with this value. For anionic surfactants with aromatic ring (such M1) the values found for the parking areas were 260−760, although the values mentioned were for symmetric $NaSO_3$ - $C_6H_4-O-(CH_2)_n-O-C_6H_4-NaSO_3$ (n = 6, 10, 12). The parking area (263−319) for M1 was comparable with these values.

The surface of the cores and the surface that could cover the surfactants present in the core−shell reactions are shown in Table 14. The amount of MA80, arising from the core reaction, was the aliquot part according to the seed used in the core−shell reaction. From the parking areas of macromonomers determined and the amounts of surfactants used in the reactions, we estimated the theoretical surface coverage of the cores in the core−shell reactions. The parking area for aerosol MA80 was 8.38×10^8 cm^2/mol,[20] and 2.53×10^8 cm^2/mol for the SLS.[14] From the results it is probable that in the reactions to synthesize C1M1, C2M1, and C2Brij latexes, the macromonomer amount used was able to cover 100% of the core's surface or even more. In the case of C1Brij, the surface coverage was only 70%.

Assuming that the macromonomers M1 and M2 have similar parking areas, due to their similar chemical composition and taking into account the ca. 2.1 times higher molecular weight of M2, it is probable that the surface coverage of core latexes in the reactions with M2 macromonomer reactions was less than 100%.

Conclusions

Two series of monodisperse core−shell latexes were prepared with functionalized macromonomers covalent-

ly bonded to their surface. The surface strong and weak acid groups were determined. The surface charge densities of latexes were low; their increases compared to the cores were mainly due to the weak acid groups of macromonomers. The existence of a hairy layer on the surface of the particles was proved for all synthesized latexes. The length of spacers determined by PCS and by DCP was ca. 3.5−4.5 nm.

The colloidal stability of the latexes, determined in terms of CCC, was lower than the expected one, corresponding to the low surface charge of the latexes. The improvement of CCC due to the presence of spacers was not confirmed, because the indifferent electrolyte used during the CCC measurements not only modified the electrostatic repulsion of the charged surfaces of the particles but also forced the spacers to collapse to the surface, decreasing their steric hindrance efficiency.

The surface coverage of cores in the core−shell reactions estimated according to the amount of emulsifiers and macromonomer used in the polymerization reactions showed that the amount of macromonomer used was not always enough to cover the core 100%.

Acknowledgment. This work is supported by the COMISIÓN INTERMINISTERIAL DE CIENCIA Y TECNOLOGÍA (CICYT), project MAT96-1035-CO3-01 and EUSKO JAURLARITZA (Fondo de Cooperación Euskadi-Aquitania). The authors would like to thank the Grupo de Fisica de Fluidos y Biocoloides, Universidad de Granada (Spain) for the electrophoretic mobility measurements. A. Búcsi thanks the EUSKO JAURLARITZA for the postdoctoral grant. Finally, we would like to express our gratitude to Dr. P. D. Armitage for revising the manuscript.

References and Notes

(1) Singer, J. M.; Plotz, C. *Am. J. Med.* **1956**, *21*, 888.
(2) Bastos, D.; Santos, R.; Forcada, J.; Hidalgo-Alvarez, R.; de las Nieves, F. J. *Colloids Surf. A: Physicochem. Eng. Asp.* **1994**, *92*, 137.
(3) Peula, J. M.; Hidalgo-Alvarez, R.; Santos, R.; Forcada, J.; de las Nieves, F. J. *J. Mater. Sci.: Mater. Med.* **1995**, *6*, 779.
(4) Sarobe, J.; Forcada, J. *Colloid Polym. Sci.* **1996**, *274*, 8.
(5) Sarobe, J.; Miraballes, I.; Molina, J. A.; Forcada, J.; Hidalgo-Alvarez, R. *Polym. Adv. Technol.* **1996**, *7* (9), 749.
(6) Santos, R.; Forcada, J. *Prog. Colloid Polym. Sci.* **1996**, *100*, 87.
(7) Eaton, P.; Cooper, G.; Johnson, R.; Mueller, R. *J. Org. Chem.* **1972**, *37*, 1947.
(8) Unzueta, E.; Forcada, J. *Polymer* **1995**, *36*, 1045.
(9) Santos, R. M.; Forcada, J. *J. Polym. Sci., Part A: Polym. Chem.* **1997**, *35*, 1605.
(10) Ottewill, R. H.; Shaw, N. J. *Discuss. Faraday Soc.* **1966**, *42*, 154.
(11) Reerink, H.; Overbeek, J. Th. G. *Discuss. Faraday Soc.* **1954**, *18*, 74.
(12) Ottewill, R. H. *J. Colloid Interface Sci.* **1977**, *58*, 357.
(13) Napper, Donald H. *Polymeric Stabilization of Colloidal Dispersions*; Academic Press: London, 1983.
(14) Rosen, Milton J. *Surfactants and Interfacial Phenomena*; John Wiley & Sons: New York, 1989.
(15) Gnanou, Y. *Indian J. Technol.* **1993**, *31*, 317.
(16) Nagasaki, Y.; Ogawa, R.; Yamamoto, S.; Kato, M.; Kataska, K. *Macromolecules* **1997**, *30*, 6489.
(17) Scholz, C.; Iijima, M.; Nagasaki, Y.; Kataoka, K. *Macromolecules* **1995**, *28*, 7295.
(18) Tsaur, L.; Fitch, R. M. *J. Colloid. Interface Sci.* **1987**, *115*, 450.
(19) Vanderhoff, J. W. Well-Characterized Monodispersed Polystyrene Latexes, as Model Colloids. In *Emulsion Polymer and Emulsion Polymerization*; [Basset, D. P., et al., Eds.; American Chemical Society: Washington, DC, 1981.
(20) Aranzazu Zamora, L. Efecto de los Parámetros de Reacción sobre los Fenómenos de Nucleación y Coagulación en Copolimerización en Emulsión. Ph.D. Thesis, Universidad del País Vasco/EHU, San Sebastián, Spain 1991.

MA971434Q